HHS Public Access

Author manuscript

*Circ Arrhythm Electrophysiol*. Author manuscript; available in PMC 2018 June 01.

Published in final edited form as:

*Circ Arrhythm Electrophysiol*. 2017 June ; 10(6): . doi:10.1161/CIRCEP.117.005084.

# Adult Ventricular Myocytes Segregate KCNQ1 and KCNE1 to Keep the $I_{Ks}$ Amplitude in Check until when Larger $I_{Ks}$ Is Needed

**Min Jiang, PhD**[1,2], **Yuhong Wang, PhD**[1,3], and **Gea-Ny Tseng, PhD**[1]

[1]Department of Physiology & Biophysics, Virginia Commonwealth University, Richmond, VA

[2]Institute of Medicinal Biotechnology, Chinese Academy of Medical Sciences & Peking Union Medical College

## Abstract

**Background—**KCNQ1 and KCNE1 assemble to form the slow delayed rectifier ($I_{Ks}$) channel critical for shortening ventricular action potentials during high β-adrenergic tone. However, too much $I_{Ks}$ under basal conditions poses an arrhythmogenic risk. Our objective is to understand how adult ventricular myocytes regulate the $I_{Ks}$ amplitudes under basal conditions and in response to stress.

**Methods and Results—**We express fluorescently-tagged KCNQ1 and KCNE1 in adult ventricular myocytes, and follow their biogenesis and trafficking paths. We also study the distribution patterns of native KCNQ1 and KCNE1, and their relationship to $I_{Ks}$ amplitudes, in chronically stressed ventricular myocytes, and use COS-7 cell expression to probe the underlying mechanism. We show that KCNQ1 and KCNE1 are both translated in the perinuclear region but traffic by different routes, independent of each other, to their separate subcellular locations. KCNQ1 mainly resides in the junctional sarcoplasmic reticulum (jSR) while KCNE1 resides on the cell surface. Under basal conditions, only a small portion of KCNQ1 reaches the cell surface to support the $I_{Ks}$ function. However, in response to chronic stress, KCNQ1 traffics from jSR to the cell surface to boost the $I_{Ks}$ amplitude in a process depending on Ca binding to calmodulin.

**Conclusions—**In adult ventricular myocytes KCNE1 maintains a stable presence on the cell surface, while KCNQ1 is dynamic in its localization. KCNQ1 is largely in an intracellular reservoir under basal conditions, but can traffic to the cell surface and boost the $I_{Ks}$ amplitude in response to stress.

### Keywords

potassium channels; calmodulin; calcium; stress; confocal imaging; two dimensional; protein trafficking; fluorescent protein; repolarization reserve

**Correspondence:** Gea-Ny Tseng, PhD, Department Physiology & Biophysics, Virginia Commonwealth University, 1101 E. Marshall St., Box 980551, Richmond, VA 23298, Tel: 804-827-0811, Fax: 804-828-7382, gtseng@vcu.edu.

[3]Current address: Chinese Academy of Medical Sciences & Peking Union Medical College, Beijing, China

**Disclosures:** None.

## Introduction

The slow delayed rectifier ($I_{Ks}$) channel is composed of pore-forming KCNQ1 channel and modulatory KCNE1 subunits[1]. $I_{Ks}$ functions as 'repolarization reserve' in ventricular myocytes[2]. Under basal conditions, $I_{Ks}$ has small amplitudes and activates slowly. Other larger and faster-activating potassium currents are responsible for repolarizing ventricular action potentials[3]. However, when β-adrenergic tone is high[4], $I_{Ks}$ becomes larger and activates faster. Enhanced $I_{Ks}$ is critical for shortening ventricular action potential duration in the face of tachycardia and increased L-type Ca current ($I_{CaL}$), allowing sufficient diastolic intervals for chamber filling[4]. Loss-of-function mutations in KCNQ1 leads to long QT syndrome type-1, which poses a high risk for ventricular fibrillation when β-adrenergic tone is high[5]. On the other hand, gain-of-function mutations in KCNQ1 have been linked to arrhythmogenic short QT syndrome type-2 and familial atrial fibrillation[6]. These clinical observations highlight the importance of keeping the $I_{Ks}$ amplitude in check under basal conditions, while allowing upward adjustment when larger $I_{Ks}$ is needed.

$I_{Ks}$ remodeling in diseased hearts may contribute to acquired arrhythmia. $I_{Ks}$ is downregulated in canine models of subacute[7] and chronic[8] myocardial infarction, contributing to acquired LQT. On the other hand, $I_{Ks}$ is upregulated in a canine model of non-ischemic cardiomyopathy[9], and in atrial myocytes from patients with chronic atrial fibrillation[10]. Whether diseased conditions may alter the subcellular distribution of $I_{Ks}$ components, and subsequently the $I_{Ks}$ amplitude, has not been investigated.

No lone KCNQ1 currents have been described for cardiac myocytes, and KCNE1 by itself does not have channel-forming capability. Therefore, KCNQ1 and KCNE1 are obligatory partners in forming the $I_{Ks}$ channels. A logic expectation is that KCNQ1 and KCNE1 should be well colocalized on myocyte surface to conduct $I_{Ks}$. However, our observations from guinea pig ventricular myocytes indicate that this is not the case: KCNQ1 exhibits a striation pattern along the z-lines, while KCNE1 is on the peripheral surface[11]. The mechanism for KCNQ1 and KCNE1 segregation, and its implication for the control of $I_{Ks}$ amplitude in normal and diseased hearts are not clear. The current study is designed to address these questions.

## Methods

### Molecular constructs

Fluorescent protein-tagged KCNQ1 and KCNE1 (Q1-GFP and E1-dsR, in plasmids or adenoviruses) have been described[11]. Angiotensin type-1 receptor (AT1R), Ca-binding deficient calmodulin ($CaM_{1234}$), and GFP-nanobody (Nb) were gifts from Drs. Y-F Xu, G. S. Pitt and B. Collins, respectively.

### Animal experiments

Three animal species were used: (1) canine: mongrel, 7, (2) guinea pig: 16, and (3) spontaneously hypertensive rat (SHR): 9. Canine as a large mammalian model has cardiac electrophysiological properties closely mimicking those of human. Guinea pig was the original model we used to study subcellular distribution of KCNQ1 and KCNE1. Old SHR

is our animal model of chronic hypertension/hypertrophy where a dramatic change in KCNQ1 distribution is observed that accounts for the increase in $I_{Ks}$. Animal procedures were in accordance with institutional guidelines (VCU IACUC protocol # 10294). The procedures of ventricular myocyte isolation, culture and adenovirus infection have been described[11].

### COS-7 culture and transfection

COS-7 cell culture and transient plasmid transfection have been described previously[11].

### GFP-Nb production and coimmunoprecipitation

GFP-Nb production was based on a published protocol[12]. GFP-Nb and DsR rabbit antibody conjugated to agarose-beads were used to immunoprecipitate Q1-GFP and E1-dsR expressed in myocytes.

### Separation of sarcoplasmic reticulum and sarcolemmal vesicles

The procedure was based a published protocol[13].

### Fluorescence in-situ hybridization of mRNAs

We used ‘QuantiGene ViewRNA ISH Cell Assay kit’ from Affymetrix to detect Q1-GFP and E1-dsR mRNAs along with the GFP and dsR protein fluorescence signals in single cardiac myocytes.

### Confocal microscopy

We used Zeiss 710 confocal microscope to image (immuno)fluorescence signals in fixed cells or to monitor Q1-GFP mobility in live cells by fluorescence recovery after photobleaching (FRAP).

### Statistical analysis

Statistical analysis was done using SigmaStat v 2. Comparison between 2 groups was done using unpaired t-test. Multiple-group comparison was done using one-way ANOVA, and if significant difference was detected, followed by pairwise comparison with Tukey’s test. Absolute p values are reported unless $p < 0.001$.

### Supplemental material

Expanded methods are presented in the Supplemental Material.

## Results

### KCNQ1 and KCNE1 are largely segregated in canine ventricular myocytes

Canine ventricular myocytes express functional $I_{Ks}$ (Fig. 1A). Fig. 1B shows that while KCNE1 is distributed on the peripheral surface, KCNQ1 exhibits a prominent striation pattern in the myocyte center. Selected cross-section views (XZ plane images reconstructed from z-stacks) do show that the two overlap on the peripheral surface in a patchy manner (* in Fig. 1B). Fig. 1C shows that the KCNQ1 and KCNE1 distribution patterns in canine

ventricular myocardium are very similar to those observed in isolated myocytes, ruling out the influence of cell isolation on KCNQ1 and KCNE1 distribution. We further use adenoviruses to express GFP tagged-KCNQ1 and dsRed tagged-KCNE1 (Q1-GFP and E1-dsR) in canine ventricular myocytes, to directly observe their distribution without using Abs. Q1-GFP and E1-dsR have been validated in terms of their channel function and trafficking patterns[11]. Fig. 1D shows that their distribution patterns are very similar to those of their native counterparts, ruling out the possibility of artifacts in immunofluorescence signals. These observations, along with those from guinea pig[11] and rat (described below), indicate a generalized $I_{Ks}$ property in adult ventricular myocytes: KCNQ1 and KCNE1 are largely segregated into different subcellular compartments. Videos #1 and #2 provide 3D visualization of native KCNQ1 and KCNE1 in guinea pig and canine ventricular myocytes, respectively.

How is the segregation between KCNQ1 and KCNE1 accomplished? We consider two scenarios. First, KCNQ1 and KCNE1 assemble into $I_{Ks}$ channels early during biogenesis as previously proposed[14, 15], and reach the cell surface together. After reaching the cell surface the assemblies dissociate[16], with KCNE1 and a small portion of KCNQ1 staying on the surface while the majority of KCNQ1 entering a striation compartment. Second, newly translated KCNQ1 and KCNE1 traffic to their separate subcellular destinations, with only a portion of the two assembled into $I_{Ks}$ channels after they have reached the surface.

## KCNQ1 and KCNE1 are segregated early during biogenesis

To differentiate between these two possibilities, we incubate canine ventricular myocytes with adenoviruses harboring Q1-GFP and E1-dsR for different durations (6–48 hr). At specified times, myocytes are fixed and the distribution patterns of Q1-GFP and E1-dsR are examined. The beginning of adenovirus incubation serves to synchronize their translation. By fixing myocytes at different time points, we can deduce where the two originate and whether they travel together or separately. To avoid overexpressing Q1-GFP or E1-dsR, which may cause non-native trafficking patterns, we use ~$1\times10^7$ plaque-forming units (PFU) per ml for Adv-Q1-GFP and ~$0.5\times10^7$ PFU/ml for Adv-E1-dsR during incubation. Fig. S1 shows that, on average, Q1-GFP and E1-dsR are expressed at levels of 50 – 100% of their native counterparts in the myocytes.

We detect Q1-GFP and E1-dsR by indirect immunofluorescence, which facilitates target detection by amplifying the signals. This is particularly important during early time points when protein expression levels are low. Negative control (omitting primary Abs, Fig. 2A) and positive control (intrinsic fluorescence signals, Fig. 2C) confirm the authenticity of the immunofluorescence signals. We carry out 7 independent experiments. The key observations are similar. For illustration purpose, we focus on one experiment (Fig. 2B). Quantitative results are presented in Fig. S2.

The earliest time point when Q1-GFP and E1-dsR can be consistently detected is 10 hr. Both appear in the perinuclear zone. For both, the perinuclear zone signals increase from 10 to 18 hr and then decline. Q1-GFP signals spread from the perinuclear zone to other cellular regions in a striation pattern along the z-lines. Newly translated Q1-GFP is rarely detected in vesicular compartments. On the other hand, E1-dsR enters a prominent vesicular

compartment that peaks at 18 hr and then declines. Q1-GFP and E1-dsR signals in the cell periphery gradually increase from 18 to 36 hrs. The % of signals in cell periphery is higher for E1-dsR than Q1-GFP. A quasi-steady state is reached after 36 hr of incubation. Videos #3 - #5 provide 3D visualization of Q1-GFP and E1-dsR distribution patterns in canine myocytes that have been incubated with adenoviruses for 18, 24, and 36 hr. In some cases (e.g. the18 hr myocyte in video #3), Q1-GFP and E1-dsR originate from around different nuclei in the same myocyte. Furthermore, Q1-GFP and E1-dsR expressed separately exhibit the same distribution patterns as when they are coexpressed (Fig. S3). These data indicate the independent nature of biogenesis and trafficking of Q1-GFP and E1-dsR in adult ventricular myocytes.

## E1-dsR travels by the 'conventional secretory pathway' but Q1-GFP does not

To understand how newly translated Q1-GFP and E1-dsR travel in adult ventricular myocytes, we compare their distribution patterns with those of key organelles in the conventional, Golgi-dependent, secretory pathway[17]. The organization of conventional secretory pathway has not been systematically examined in adult ventricular myocytes but has been well characterized for COS-7 cells[17]. Fig. 3A shows that protein translation sites (nuclear envelope, 'NE', and rough endoplasmic reticulum,' rER') can be marked by ER-resident proteins, calnexin and binding protein 'BiP'. Newly translated proteins are transported from ER to Golgi through an intermediate compartment, marked by ERGIC-53. N-glycosylated proteins are processed during transit through the Golgi apparatus, becoming complex-glycosylated and capable of binding wheat germ agglutinin 'WGA'. Golgi-processed proteins traffic to the plasma membrane in WGA-positive structures. Finally, βCOP marks COPI vesicles that mediate Golgi-to-ER and intra-Golgi transports.

Fig. 3B shows that in adult ventricular myocytes calnexin and BiP, now termed sarco/endoplasmic reticulum (SR/ER) markers, exhibit a striation pattern along the z-lines, suggesting that junctional SR (jSR) may be active in protein translation/folding. ERGIC-53 positive vesicles are widely distributed in myocytes. There are large round structures aligned with the myocyte longitudinal axis positive for both WGA and βCOP, suggesting that these are the Golgi apparatus and post-Golgi structures.

Fig. 3C shows that E1-dsR vesicles are positive for both WGA and βCOP, indicating that newly translated E1-dsR enters trans-Golgi network 'TGN' and post-Golgi structures, i.e. it traverses the conventional secretory pathway. On the other hand, there is no overlap between Q1-GFP and WGA or βCOP (Fig. 3D), suggesting that newly translated Q1-GFP travels through a distinctly different pathway[18].

## Both Q1-GFP and E1-dsR are translated in the perinuclear zone

Is it possible that the distinctly different distribution patterns of newly translated Q1-GFP and E1-dsR reflect separate translation sites? To address these questions we use fluorescence in situ hybridization to detect Q1-GFP and E1-dsR mRNAs (by red and green fluorophore-conjugated probes, respectively) and their protein products (by intrinsic fluorescence) in the same myocyte. To avoid conflicts in fluorescence signals, we express Q1-GFP and E1-dsR separately. These experiments are conducted on adult ventricular myocytes from young

spontaneously hypertensive rats (SHRs), which express functional $I_{Ks}$ (see below). Fig. S4 shows that the distribution patterns of newly translated Q1-GFP and E1-dsR in SHR myocytes are similar to those in canine myocytes. Importantly, Q1-GFP and E1-dsR expressed separately exhibit the same distribution patterns as when they are coexpressed in SHR myocytes.

Fig. 4A shows that Q1-GFP mRNA clusters around nuclei in the space between nuclei and the cell membrane. Q1-GFP protein is detected in the perinuclear zone, and in regions away from the nuclei where no Q1-GFP mRNA signals are detected. Video #6 depicts 3D visualization of Q1-GFP mRNA and protein in this myocyte. Similar observations are obtained from 13 myocytes. These data indicate that Q1-GFP is translated in the perinuclear zone and spreads to other cellular regions in a striation pattern.

E1-dsR mRNA also clusters around nuclei in the space between nuclei and cell membrane (Fig. 4B). E1-dsR vesicles are detected in regions where no E1-dsR mRNA is detected (video #7). Similar observations are obtained from11 myocytes. These observations indicate that E1-dsR is translated in the perinuclear zone and spreads to other cellular regions in vesicles.

## The striation pattern of KCNQ1 represents localization in junctional SR

The striation pattern of native KCNQ1 and Q1-GFP in adult ventricular myocytes may represent t-tubule and/or jSR localization. Distinction between the two has important implications: KCNQ1 channels in the t-tubule may contribute to surface electrical activity, while KCNQ1 in jSR likely serves as an intracellular reservoir. Fig. 5A shows that KCNQ1 maintains its striation pattern in myocytes where t-tubules are missing. On the other hand, Fig. 5B shows that the striation pattern of native KCNQ1 coincides with those of SR proteins: ryanodine receptor type 2 (RyR2), junctophilin-2 (JPH-2), SR/ER Ca pump (SERCA2a), calsequestrin 2 (CSQ2), and calnexin. The distance between t-tubule and jSR membranes is only 10–25 nm, beyond the detection limit of confocal and even high-resolution microscopy. Therefore, we use two alternative approaches to probe the subcellular environments of Q1-GFP/native KCNQ1 and E1-dsR/native KCNE1 in adult ventricular myocytes.

First, we immunoprecipitate Q1-GFP and E1-dsR along with their binding partners from myocytes. This allows us to deduce their immediate subcellular environment based on their binding partners. The top 2 rows of Fig. 5C confirm the effectiveness of our co-immunoprecipitation approach: GFP nanobody (Nb) pulls down E1-dsR associated with Q1-GFP, while dsR rabbit pAb pulls down Q1-GFP associated with E1-dsR. The middle 5 rows of Fig. 5C show that Q1-GFP can be co-immunoprecipitated with SR/ER markers: RyR2, SERCA2a, CSQ2, calnexin, and JPH-2. Importantly, CSQ2 is an SR/ER luminal protein. The fact that CSQ2 can be co-immunoprecipitated with Q1-GFP indicates that Q1-GFP is embedded in the SR/ER membrane with its extracellular domain facing the SR/ER lumen accessible to CSQ2. On the other hand, E1-dsR cannot be co-immunoprecipitated with RyR2, CSQ2 or JPH-2. E1-dsR can be co-immunoprecipitated with calnexin, reflecting nascent E1-dsR being translated in the rER. We also detect very faint SERCA2a signal in the

dsR pAb immunoprecipitate, at a level much weaker than SERCA2a signal in the GPF Nb immunoprecipitate. The remaining panels of Fig. 5C will be discussed later (in *Discussion*).

The second approach is to separate the SR/ER and sarcolemmal (SL) compartments and quantify their contents of native KCNQ1 and KCNE1. These experiments are conducted on guinea pig hearts using a previously described protocol[13]. Membrane vesicles prepared from whole heart homogenates are subjected to Ca-oxalate loading through the membrane Ca-pump activity. Because the SR/ER vesicles express a higher Ca-pump activity than SL vesicles, a brief loading duration (5 min at 36°C) will preferentially load the SR/ER vesicles with Ca-oxalate, making them heavier than the SL vesicles. This allows separation between the two by ultracentrifugation through sucrose gradients. The resulting SL and SR gradients are noted on top of Fig. 5D, based on the distribution patterns of SR/ER markers (RyR2, SERCA2a, and calnexin) and SL markers (NCX*, glycosylated Na/Ca exchanger, and Na-K-pump). The distribution of native KCNQ1 follows the SR/ER markers, while the distribution of native KCNE1 follows the SL markers. Fig. 5C and 5D together provide direct evidence that KCNQ1 (as Q1-GFP or native counterpart) resides in the SR/ER compartment, but KCNE1 is mainly on the cell surface.

## KCNQ1 can move among cellular areas within the SR/ER compartment

In interphase cells the ER is a single organelle with interconnecting membranes throughout the cells[17]. If Q1-GFP is in the SR/ER compartment of adult ventricular myocytes, it may be able to move from one region to another through the SR/ER membranes. We test this possibility using the technique of fluorescence recovery after photobleaching (FRAP). We bleach a small area in the center of canine ventricular myocyte where Q1-GFP is in clear striations. Q1-GFP can move from unbleached areas to replenish the fluorescence in the bleached area, and the recovered fluorescence resumes the original striation pattern (n=41, Fig. 6Aa, and video #8). These data support the above scenario: KCNQ1 resides in the SR/ER membranes. The striation pattern reflects its high abundance in the jSR regions.

The mobility of Q1-GFP in ventricular myocytes is much slower than that in the ER compartment of COS-7 cells (Fig. 6A, c). Protein mobilities are influenced by their sizes: large multiple-protein complexes move slower than small protein complexes. Fig. 5C reveal that Q1-GFP can interact with multiple SR/ER proteins, possibly forming one or more forms of macromolecular complexes. This may slow its mobility in ventricular myocytes. To test this possibility, we coexpress JPH-2, one of the strongest Q1-GFP binding partners, in COS-7 cells and analyze its effect on Q1-GFP mobility. Panels ‘a’ and ‘b’ in Fig. 6B confirm that JPH-2 can be co-immunoprecipitated with Q1-GFP, and JPH-2 puncta (representing ER-PM junctions) overlap with Q1-GFP in the ER reticulum. JPH-2 coexpression significantly slows Q1-GFP mobility in the ER compartment (prolonging the time constant of fluorescence recovery, $\tau_{recovery}$, although no change in the percent of stead-state Q1-GFP recovery, % mobile, Fig. 6B, c - e).

These data support the notion that in ventricular myocytes KCNQ1 is stabilized by extensive interactions with SR/ER resident proteins. On the other hand, cell peripheral Q1-GFP recovers at a significantly faster rate than cell center, SR/ER-resident Q1-GFP (Fig. 6A, b

and c). This difference suggests that cell peripheral Q1-GFP forms smaller molecular complexes than its counterpart in the SR/ER compartment.

## KCNQ1 reservoir in the SR/ER compartment endows adult ventricular myocytes with the ability to increase $I_{Ks}$ amplitude in times of need

Can KCNQ1 move from the intracellular SR/ER reservoir to cell surface and boost the $I_{Ks}$ amplitude when a larger $I_{Ks}$ is needed? Data presented in Fig. 7 support such a scenario. SHR ventricular myocytes express native KCNQ1, KCNE1 and functional $I_{Ks}$ channels, whose currents can be separated from other much larger currents, such as transient outward '$I_{to}$', as HMR1556-sensitive currents[19]. Old SHRs (SO, 22–24 months of age) exhibit symptoms of heart failure: severe interstitial fibrosis, left atrial enlargement and thrombosis (indicative of atrial fibrillation) (Fig. 7A), as well as ventricular wall-thinning and chamber dilatation. The $I_{to}$ current density in left ventricular epicardial (LV Epi) myocytes from SO is markedly reduced than those from young SHR (SY, 4–6 months of age) (data not shown). However, the $I_{Ks}$ current density is larger in LV Epi myocytes from SO than SY, while the gating kinetics is not altered (e.g. no shift in the voltage-dependence of $I_{Ks}$ activation, Fig. 7B). Immunoblot experiments on whole tissue lysates from LV Epi samples show that the KCNQ1 protein level is only modestly elevated in SO than SY, but KCNE1 protein level is reduced in SO than SY, especially in severely hypertrophied hearts (Fig. 7C). Therefore, the changes in KCNQ1 and KCNE1 protein levels cannot explain the marked increase in $I_{Ks}$ current density in SO myocytes. We monitor the distribution patterns of native KCNQ1 and KCNE1 in the SHR myocytes (Fig. 7D). While KCNE1 is stable on the peripheral surface of both SY and SO myocytes, the patterns of KCNQ1 are dramatically different. In SY myocytes KCNQ1 exhibits clear striations along the z-lines, the same as KCNQ1 in canine and guinea pig myocytes (Fig. 1)[11], indicating jSR localization. In SO myocytes KCNQ1 disappears from the jSR compartment but clusters to the peripheral surface. As a result, the degree of KCNQ1/KCNE1 colocalization in myocyte periphery is significantly higher in SO than SY myocytes (Fig. 7E).

The above data are not uniquely SHR phenomenon. Fig. S5 illustrates that the increase in $I_{Ks}$ amplitude in chronically stressed canine ventricular myocytes (cardiomyopathy induced by chronic premature ventricular contractions, PVC) is accompanied by a similar shift of KCNQ1 from the SR to the SL compartment.

## Persistent AT1R stimulation promotes KCNQ1 trafficking to cell surface in a Ca- and calmodulin-dependent manner

What may trigger KCNQ1 to move from jSR to cell surface? It has been shown that in old SHR heart local angiotensin II (Ang II) levels are elevated, leading to a persistent activation of angiotensin type 1 receptor (AT1R) and its downstream signaling cascades[20]. Chronic ventricular pacing in the canine heart also causes local Ang II elevations and AT1R activation[21]. Therefore, we test the effect of persistent AT1R stimulation on $I_{Ks}$ channel function and KCNQ1/KCNE1 distribution. The experiments are conducted in COS-7 cells coexpressing AT1R and recombinant $I_{Ks}$ (KCNQ1 plus KCNE1). Ang II pretreatment causes an increase in the $I_{Ks}$ density (Fig. 8Aa) and a negative shift in the threshold voltage of $I_{Ks}$ activation (Fig. 8Ab). The latter change can be explained by an increase in cell surface

KCNQ1 without a concomitant increase in cell surface KCNE1. Indeed, KCNQ1 expressed alone responds to Ang II pretreatment with a prominent increase in current density without shifting the threshold of activation (Fig. 8A a–c). Biotinylation experiments confirm that Ang II pretreatment increases cell surface KCNQ1 but not KCNE1 (Fig. 8B, left 2 panels).

AT1R stimulation can activate phospholipase C, which hydrolyzes membrane phosphatidylinositol 4,5-biphosphate ($PIP_2$) producing inositol 1,4,5-triphosphate ($IP_3$). $IP_3$ induces Ca release through $IP_3$ receptors in the SR/ER membrane, leading to $[Ca]_i$ elevation. It has been shown that $[Ca]_i$ elevation can increase native $I_{Ks}$ amplitude in guinea pig ventricular myocytes in a calmodulin (CaM)-dependent manner[22]. This occurs through Ca binding to CaM constitutively associated with the C-terminus of KCNQ1[23, 24]. To test whether this signaling cascade is involved in the increase in cell surface KCNQ1, we test the effects of two interventions on the $I_{Ks}$ response to AT1R stimulation: (1) preventing Ca binding to CaM, by displacing the native CaM with a Ca-binding deficient CaM mutant, $CaM_{1234}$[23], through overexpression, and (2) inhibiting Ca release through $IP_3$ receptor, by including 5 uM of 2-aminoethoxydiphenyl borate '2APB'[25] during Ang II incubation. Fig. 8A, two right panels in 'c' show that both $CaM_{1234}$ overexpression and $IP_3$ receptor inhibition prevent AT1R stimulation from increasing $I_{Ks}$ current density. Biotinylation experiments show that AT1R stimulation fails to increase cell surface KCNQ1 under these two conditions (Fig. 8B, 2 right panels).

## Discussion

The following are our major findings. First, there is a general $I_{Ks}$ property in adult ventricular myocytes: most KCNQ1 is in an intracellular junctional SR reservoir revealed in microscopic experiments as striations along the z-lines, while KCNE1 is on the peripheral surface. Second, the segregation of KCNQ1 and KCNE1 begins during their biogenesis. Although both proteins are translated in the perinuclear zone, newly translated KCNQ1 and KCNE1 traffic by different routes, independent of each other, to their separate destinations. Third, KCNE1 traffics in vesicles through the conventional, Golgi-dependent pathway to reach the myocyte surface. On the other hand, FRAP experiments show that KCNQ1 can move within the SR/ER compartment in cardiac myocytes. Fourth, due to the segregation between KCNQ1 and KCNE1, under basal conditions only a small portion of KCNQ1 is on the myocyte surface, assembled with KCNE1 to support the basal $I_{Ks}$ channel function. However, chronic stress (in old SHR and chronic PVC canine models) promotes KCNQ1 exit from the SR/ER compartment. KCNQ1 moves to the myocyte surface and assembles with KCNE1 to boost the $I_{Ks}$ amplitude. Fifth, experiments in the COS-7 expression system suggest that the above KCNQ1 trafficking process depends on Ca binding to calmodulin.

### What stabilizes KCNE1 on the myocyte surface?

When expressed in COS-7 cells, cell surface KCNE1 is not stable but experiences rapid endocytosis[26]. To explore the mechanism stabilizing KCNE1 on the myocyte surface, we test whether KCNE1 interacts with scaffolding proteins known, or potentially able, to anchor KCNE1. Telethonin and four-and-half LIM-domain containing protein 2 (FHL-2) have been suggested to anchor KCNE1 in cardiac myocytes[27, 28]. $I_{Ks}$ channels cluster to caveolae in

guinea pig ventricular myocytes[29], that are stabilized by caveolin-3. Finally, α-actinin may stabilize surface proteins indirectly. We cannot detect any of these proteins in dsR pAb immunoprecipitate from myocyte lysates expressing E1-dsR. Further experimentation with a global search strategy is required to answer this question.

## Implications for the regulation of $I_{Ks}$ amplitude in adult ventricular myocytes

Ca binding to KCNQ1-associated calmodulin leads to an increase in the number of $I_{Ks}$ channels on the cell surface[22, 23]. Here we show that in adult ventricular myocytes, most KCNQ1 is in the junctional SR with its cytoplasmic C-terminal domain facing the dyadic space. KCNE1 is on the cell surface, ready to form $I_{Ks}$ channels when KCNQ1 is available. We suggest that the cyclic elevations of [Ca] in the dyadic space during cardiac action potentials serve as a trigger for KCNQ1 to exit the jSR and reach the cell surface, where it assembles with KCNE1 to support the $I_{Ks}$ function.

The most important physiological function of $I_{Ks}$ is to respond to β-adrenergic stimulation: $I_{Ks}$ becomes larger and activates faster, so that it can help shorten the ventricular action potentials. β-adrenergic stimulation increases $I_{Ks}$ by two known mechanisms: (1) accumulating $I_{Ks}$ channels in activated state during β-adrenergic-induced tachycardia (operating in seconds)[30], and (2) protein kinase A-mediated phosphorylation of $I_{Ks}$ components (operating in minutes)[31]. Live cell imaging shows that acute exposure of quiescent canine ventricular myocytes expressing Q1-GFP to β-adrenergic agonist (isoproterenol 1 uM, 37°C, up to 30 min) does not induce trafficking events. However, in *in situ* ventricular myocytes, β-adrenergic stimulation can amplify [Ca] spike in the dyadic space during E-C coupling. This can promote KCNQ1 trafficking to the cell surface, constituting a third mechanism for β-adrenergic-induced increase in $I_{Ks}$ that operates on the minutes-to-hour time scale.

Acute AT1R stimulation in canine and guinea pig ventricular myocytes induces a small and transient $I_{Ks}$ enhancement followed by a steady decline, which likely reflects PIP2 depletion following PLC activation. COS-7 expression showed prominent and consistent enhancement of KCNQ1 or $I_{Ks}$ following ≥1 hr of AT1R stimulation, due to KCNQ1 trafficking to the cell surface.

## Novelty of this study

Our study provides the following novel insights into how adult ventricular myocytes regulate their $I_{Ks}$ current amplitude to suit their needs: (1) KCNQ1 and KCNE1 are translated separately and transported in different routes, assembled into $I_{Ks}$ after reaching the cell surface. This is different from the previous view that KCNQ1 and KCNE1 assemble into $I_{Ks}$ early during biogenesis (in the ER or soon thereafter[14,15]). (2) The striation pattern of KCNQ1 in adult ventricular myocytes reflects its localization in the jSR compartment. This is different from the previous belief that KCNQ1 is localized in the t-tubule membrane. (3) Chronic stress as seen in old SHR and PVC dog can promote KCNQ1 translocation from jSR to cell surface, leading to an increase in $I_{Ks}$ in ventricular myocytes. This is different from the prevailing view that $I_{Ks}$ is downregulated in diseased heart. However, we note that $I_{Ks}$ indeed is downregulated in ventricular myocytes surviving myocardial infarction[7,8].

## Supplementary Material

Refer to Web version on PubMed Central for supplementary material.

## Acknowledgments

Confocal microscopy was performed at the Virginia Commonwealth University – Department of Neurobiology & Anatomy Microscopy Facility, supported in part by NIH-NINDS Center Core Grant 5P30NS047463. We thank Drs. Jose F. Huizar and Alex Tan for providing canine ventricular myocytes.

**Sources of Funding:** This study was supported by RO1 HL128610 and HL107294 from NIH, and 16GRNT29920012 from American Heart Association (to GNT).

## References

1. Sanguinetti MC, Curran ME, Zou A, Shen J, Spector PS, Atkinson DL, Keating MT. Coassembly of KvLQT1 and minK (IsK) proteins to form cardiac IKs potassium channel. Nature. 1996; 384:80–83. [PubMed: 8900283]
2. Sarkar AX, Sobie EA. Quantification of repolarization reserve to understand interpatient variability in the response to proarrhythmic drugs: A computational analysis. Heart Rhythm. 2016; 8:1749–1755.
3. Jost N, Virag L, Comtois P, Ordog B, Szuts V, Seprenyi G, Bitay M, Kohajda Z, Koncz I, Nagy N, Szel T, Magyar J, Kovacs M, Puskas LG, Lengyel C, Wettwer E, Ravens U, Nanasi PP, Papp JG, Varro A, Nattel S. Ionic mechanisms limiting cardiac repolarization reserve in humans compared to dogs. J Physiol. 2013; 591:4189–4206. [PubMed: 23878377]
4. Jost N, Virag L, Bitay M, Takacs J, Lengyel C, Biliczki P, Nagy Z, Bogats G, Lathrop DA, Papp JG, Varro A. Restricting excessive cardiac action potential, QT prolongation A vital role for IKs in human ventricular muscle. Circulation. 2005; 112:1392–1399. [PubMed: 16129791]
5. Choi G, Kopplin LJ, Tester DJ, Will ML, Haglund CM, Ackerman MJ. Spectrum and frequency of cardiac channel defects in swimming-triggered arrhythmia syndromes. Circulation. 2004; 110:2119–2124. [PubMed: 15466642]
6. Borggrefe M, Wolpert C, Antzelevitch C, Veltmann C, Giustetto C, Gaita F, Schimpf R. Short QT syndrome genotype-phenotype correlatoins. J Electrocardiology. 2005; 38:75–80.
7. Jiang M, Cabo C, Yao J-A, Boyden PA, Tseng G-N. Delayed rectifier K currents have reduced amplitudes and altered kinetics in myocytes from infarcted canine ventricle. Cardiov Res. 2000; 48:34–43.
8. Liu X-S, Jiang M, Zhang M, Tang D, Higgins RSD, Tseng G-N. Electrical remodeling in a canine model of ischemic cardiomyopathy. Am J Physiol. 2007; 292:H560–H571.
9. Wang Y-H, Eltit JM, Kaszala K, Tan A, Jiang M, Zhang M, Tseng G-N, Huizar JF. Cellular mechanism of premature ventricular contraction-induced cardiomyopathy. Heart Rhythm. 2014; 11:2064–2072. [PubMed: 25046857]
10. Caballero R, de la Fuente MG, Gomez R, Barana A, Amoros I, Dolz-Gaiton P, Osuna L, Almendral J, Atienza F, Fernandez-Aviles F, Pita A, Rodriguez-Roda J, Pinto A, Tamargo J, Delpon E. In humans, chronic atrial fibrillation decreases the transient outward current and ultrarapid component of the delayed rectifier current differentially on each atria and increases the slow component of the delayed rectifier current in both. J Am Coll Cardiol. 2010; 55:2346–2354. [PubMed: 20488306]
11. Wang Y-H, Zankov DP, Jiang M, Zhang M, Henderson SC, Tseng G-N. [Ca]i elevation and oxidative stress induce KCNQ1 translocation from cytosol to cell surface and increase IKs in cardiac myocytes. J Biol Chem. 2013; 288:35358–35371. [PubMed: 24142691]
12. Rothbauer U, Zolghadr K, Muyldermans S, Schepers A, Cardoso MC, Leonhardt H. A Versatile Nanotrap for Biochemical and Functional Studies with Fluorescent Fusion Proteins. Mol Cell Proteomics. 2008; 7:282–289. [PubMed: 17951627]

13. Jones LR, Besch HR Jr, Fleming JW, McConnaughey MM, Watanabe AM. Separation of vesicles of cardiac sarcolemma from vesicles of cardiac sarcoplasmic reticulum Comparative biochemical analysis of component activities. J Biol Chem. 1979; 254:530–539. [PubMed: 216677]
14. Chandrasekhar KD, Bas T, Kobertz WR. KCNE1 subunits require co-assembly with K+ channels for efficient trafficking and cell surface expression. J Biol Chem. 2006; 281:40015–40023. [PubMed: 17065152]
15. Vanoye CG, Welch RC, Tian C, Sanders CR, George AL Jr. KCNQ1/KCNE1 assembly, co-translation not required. Channels (Austin). 2010; 4:108–114. [PubMed: 20139709]
16. Jiang M, Xu X-L, Wang Y-H, Toyoda F, Liu X-S, Zhang M, Robinson RB, Tseng G-N. Dynamic partnership between KCNQ1 and KCNE1 and influence on cardiac IKs current amplitude by KCNE2. J Biol Chem. 2009; 284:16452–16462. [PubMed: 19372218]
17. Lippincott-Schwartz J, Roberts TH, Hirschberg K. Secretory protein trafficking and organelle dynamics in living cells. Ann Rev Cell Dev Biol. 2000; 16:557–589. [PubMed: 11031247]
18. Prydz K, Tveit H, Vedeler A, Saraste J. Arrivals and departures at the plasma membrane: direct and indirect transport routes. Cell Tissue Res. 2013; 352:5–20. [PubMed: 22526627]
19. Wu D-M, Jiang M, Zhang M, Liu X-S, Korolkova YV, Tseng G-N. KCNE2 is colocalized with KCNQ1 and KCNE1 in cardiac myocytes and may function as a negative modulator of IKs current amplitude in the heart. Heart Rhythm. 2006; 3:1469–1480. [PubMed: 17161791]
20. Cerbai E, Crucitti A, Sartiani L, De Paoli P, Pino R, Rodriguez ML, Gensini G, Mugelli A. Long-term treatment of spontaneously hypertensive rats with losartan and electrophysiological remodeling of cardiac myocytes. Cardiov Res. 2000; 45:388–396.
21. Ozgen N, Rosen MR. Cardiac memory: A work in progress. Heart Rhythm. 2009; 6:564–571. [PubMed: 19324320]
22. Nitta J-I, Jurukawa T, Marumo F, sawanobori T, Hiraoka M. Subcellular mechanism for Ca2+-dependent enhancement of delayed rectifier K+ current in isolated membrane patches of guinea pig ventricular myocytes. Circ Res. 1994; 74:96–104. [PubMed: 8261599]
23. Ghosh S, Nunziato DA, Pitt GS. KCNQ1 assembly and function is blocked by long-QT syndrome mutations that disrupt interaction with calmodulin. Circ Res. 2006; 98:1048–1054. [PubMed: 16556866]
24. Shamgar L, Ma L, Schmitt N, Haitin Y, Peretz A, Wiener R, Hirsch J, Pongs O, Attali B. Calmodulin is essential for cardiac IKs channel gating, assembly Impaired function in long-QT mutations. Circ Res. 2006; 98:1055–1063. [PubMed: 16556865]
25. Zima AV, Blatter LA. Inositol-1,4,5-triphosphate-dependent Ca2+ signalling in cat atrial excitation-contraction coupling and arrhythmias. J Physiol. 2004; 555:607–615. [PubMed: 14754996]
26. Xu X, Kanda VA, Choi E, Panaghie G, Roepke TK, Gaeta SA, Christini DJ, Lerner DJ, Abbott GW. MinK-dependent internalization of the IKs potassium channel. Cardiov Res. 2009; 82:430–438.
27. Furukawa T, Ono Y, Tsuchiya H, Katayama Y, Bang M-L, Labeit D, Labeit S, Inagaki N, Gregorio CC. Specific interaction of the potassium channel β-subunit minK with the sarcomeric protein T-cap suggests a T-tubule-myofibril linking system. J Mol Biol. 2001; 313:775–784. [PubMed: 11697903]
28. Kupershmidt S, Yang ICH, Sutherland M, Wells KS, Yang T, Yang P, Balser JR, Roden DM. Cardiac-enriched LIM domain protein fhl2 is required to generate IKs in a heterologous system. Cardiov Res. 2002; 56:93–103.
29. Nakamura H, Kurokawa J, Bai C-X, Asada K, Xu J, Oren RV, Zhu ZI, Clancy CE, Isobe M, Furukawa T. Progesterone regulates cardiac repolarization through a nongenomic pathway. An in vitro patch-clamp and computational modeling study. Circulation. 2007; 116:2913–2922. [PubMed: 18056530]
30. Silva J, Rudy Y. Subunit interaction determines IKs participation in cardiac repolarization and repolarization reserve. Circulation. 2005; 112:1384–1391. [PubMed: 16129795]
31. Marx SO, Kurokawa J, Reiken S, Motoike H, D'Armiento J, Marks AR, Kass RS. Requirement of a macrocmolecular signaling complex for β adrenergic receptor modulaiton of the KCNQ1-KCNE1 potassium channel. Science. 2002; 295:496–499. [PubMed: 11799244]

**WHAT IS KNOWN**

- The pore-forming component and auxiliary subunit of the slow delayed rectifier ($I_{Ks}$) channel, KCNQ1 and KCNE1 respectively, are obligatory partners in cardiac myocytes, because when existing alone they conduct little (KCNQ1) or no (KCNE1) current.
- The $I_{Ks}$ channel functions as the major 'repolarization reserve' in human ventricular myocytes, i.e. $I_{Ks}$ has a small amplitude and activates slowly under basal conditions when other larger, faster-activating repolarizing currents control the action potential duration adequately, but becomes larger and activates faster when β-adrenergic tone is high and more repolarizing currents are needed to shorten the action potential duration.

## WHAT THIS STUDY ADDS

- Under basal conditions, adult ventricular myocytes have KCNQ1 largely in an intracellular reservoir (junction SR), with only a small portion of KCNQ1 colocalized with KCNE1 on the cell surface to conduct a small $I_{Ks}$.
- Stressors such as AT1R stimulation can trigger exit of KCNQ1 from its intracellular reservoir in a Ca- and calmodulin-dependent manner to reach the cell surface, where it can assemble with KCNE1 to increase the $I_{Ks}$ amplitude.
- Chronically stressed and hypertrophied ventricular myocytes (e.g. from old spontaneously hypertensive rats or dogs exposed to chronic premature ventricular contractions) have a persistent pool of KCNQ1 on the cell surface, which boosts the $I_{Ks}$ amplitude and may be a protective mechanism when other repolarizing channels (e.g. $I_{to}$ and $I_{K1}$) are downregulated.

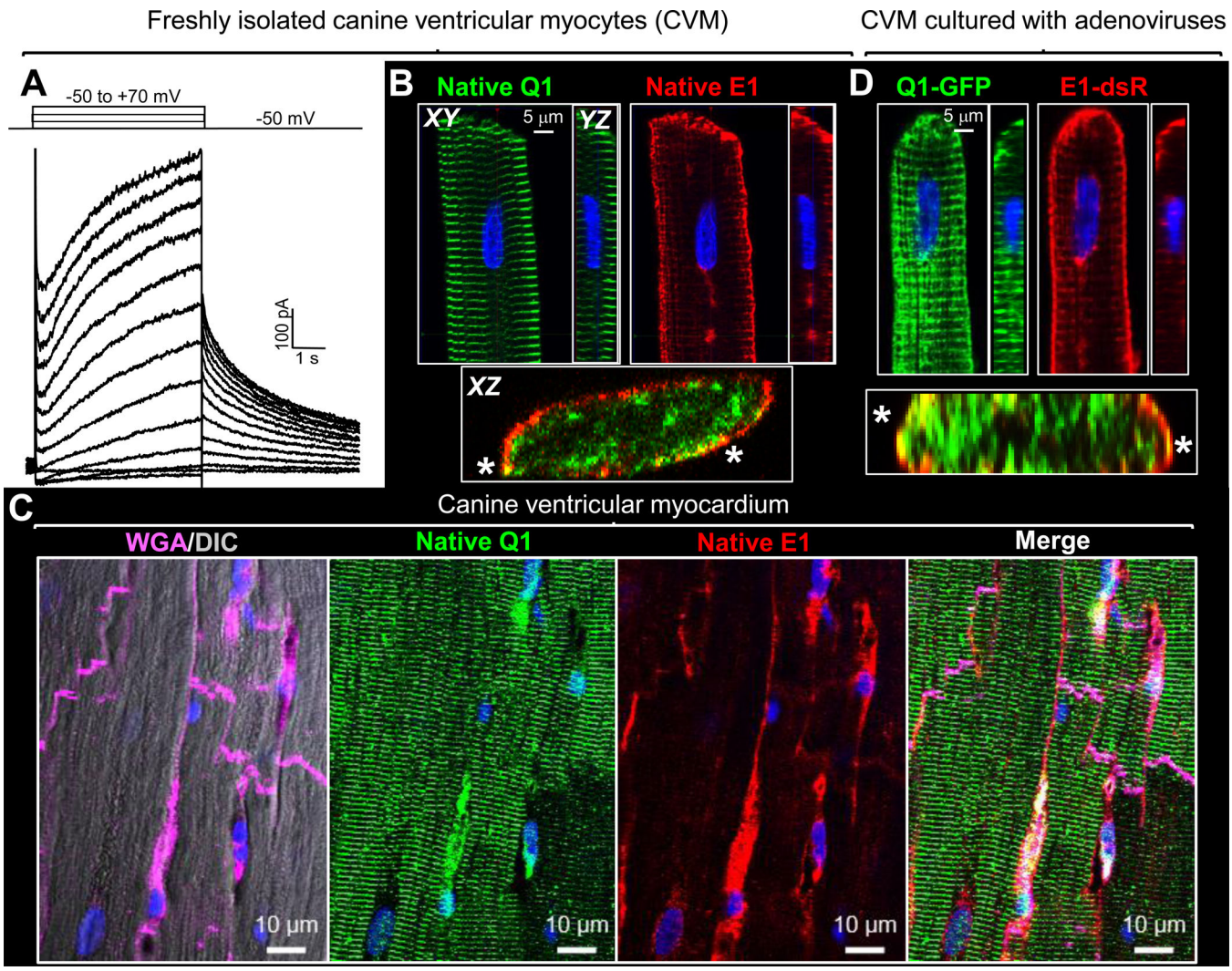


**Figure 1.**

Segregation of KCNQ1 (Q1) and KCNE1 (E1) in canine ventricular myocytes (CVMs). (**A**) $I_{Ks}$ recorded from a CVM elicited by diagrammed voltage-clamp protocol. (**B**) Immunofluorescence (IF) detection of native Q1 and E1 in CVM. (**C**) IF detection of native Q1 and E1 in canine ventricular myocardium. Wheat germ agglutinin (WGA) marks cell boundaries. DIC: differential interference contrast. (**D**) Adenovirus-mediated expression of Q1-GFP and E1-dsR in CVM. 'XY' plane images are from centers of z-stacks; YZ and XZ plane images are reconstructed from z stacks. XZ views here show merged fluorescence signals. *: Q1 and E1 overlap on myocyte peripheral surface. Nuclei stained blue with DAPI.

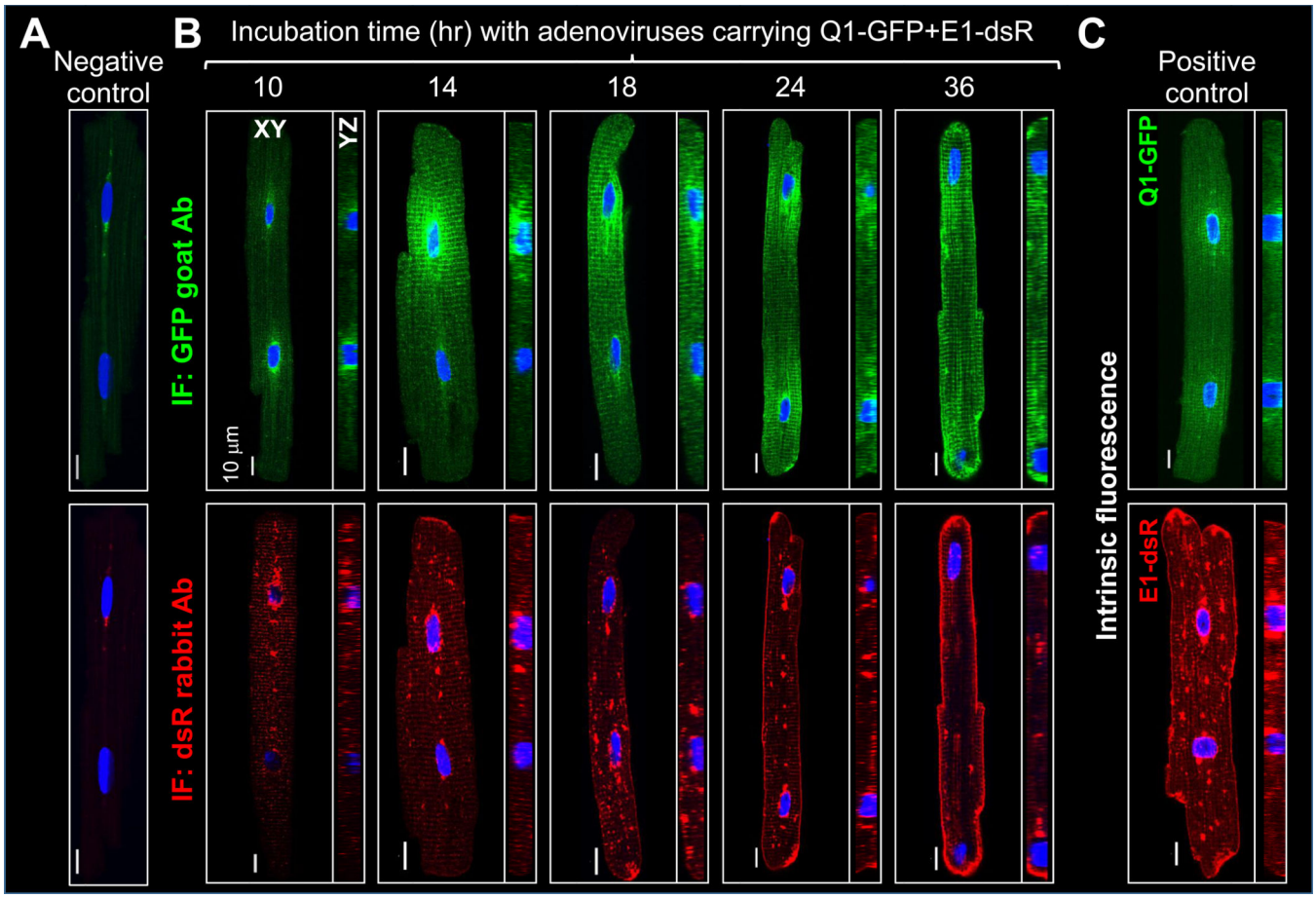


**Figure 2.**

Tracking the origin and distribution of newly translated Q1-GFP and E1-dsR in canine ventricular myocytes. CVMs are incubated with Adv-Q1-GFP and Adv-E1-dsR for different durations, fixed, and immunostained with GFP goat Ab/Alexa488 anti-goat and dsR rabbit Ab/Alexa 568 anti-rabbit. (**A**) Negative control (omitting primary Abs in a myocyte incubated with adenoviruses for 10 hr). (**B**) Distribution patterns of Q1-GFP and E1-dsR after different adenovirus incubation times. (**C**) Positive control (intrinsic Q1-GFP and E1-dsR fluorescence signals in CVM incubated with adenoviruses for 24 hr).

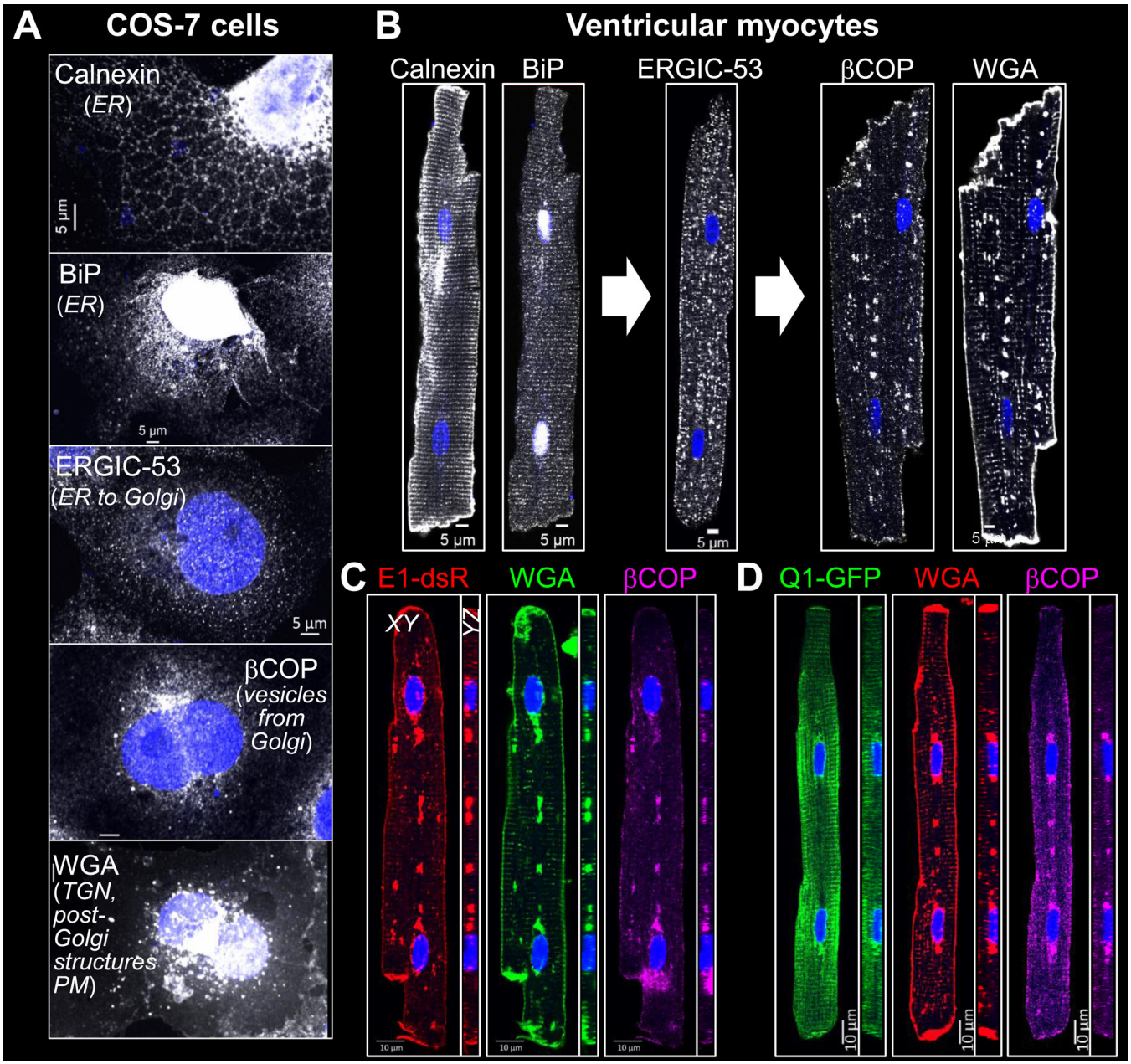


**Figure 3.**

Distribution patterns of organelles in the conventional secretory pathway and implication for the trafficking paths of E1-dsR and Q1-GFP in adult ventricular myocytes. (**A**) and (**B**) (Immuno)fluorescence images of COS-7 cells and canine ventricular myocytes detected by antibodies targeting specified organelle markers or by Alexa-conjugated WGA. (**C**) and (**D**) Comparing E1-dsR and Q1-GFP distribution patterns with those of WGA and βCOP in canine ventricular myocytes incubated with adenoviruses for 18 hr.

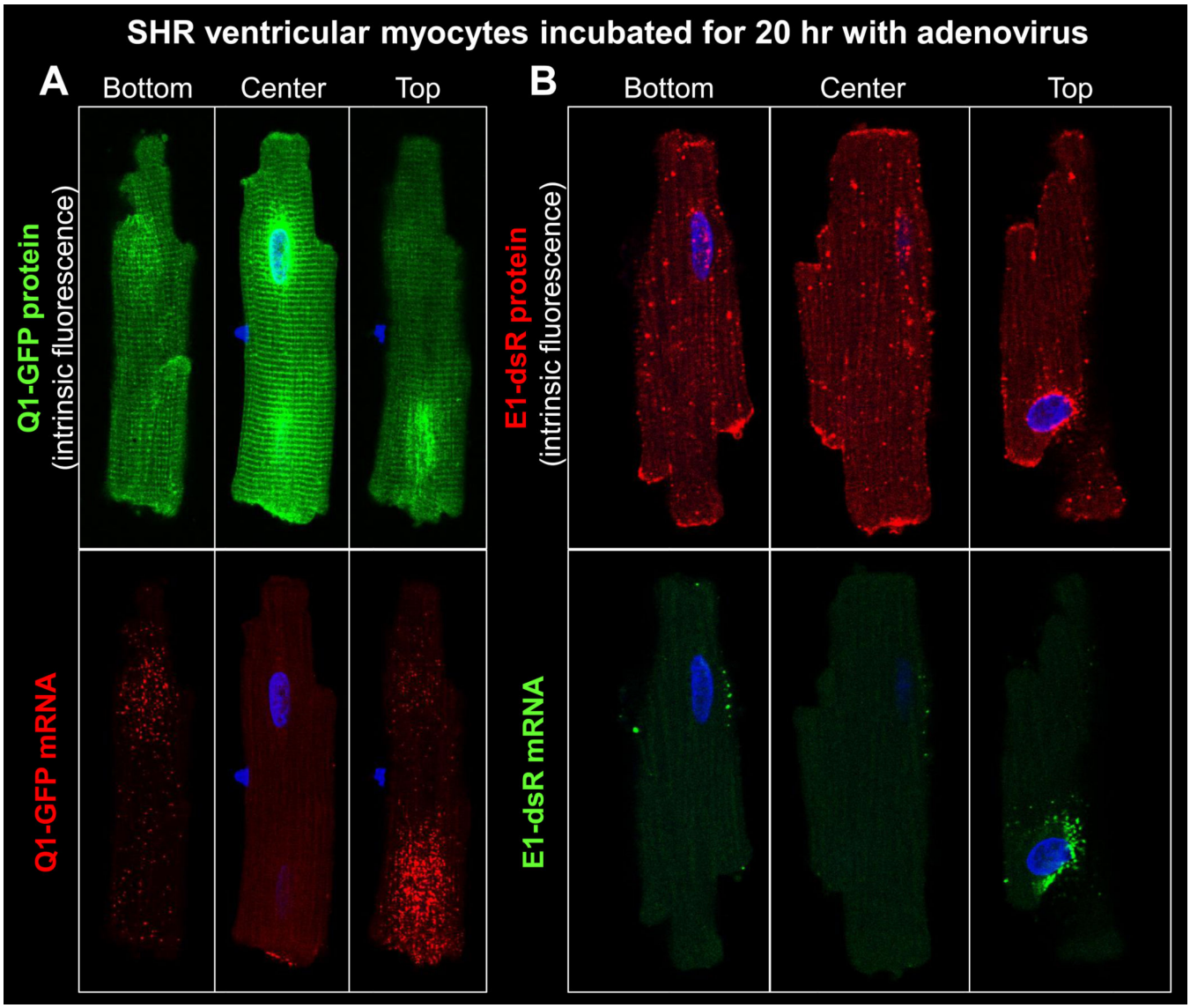


**Figure 4.**

Comparing distribution patterns of mRNA and newly translated protein of Q1-GFP (A) and E1-dsR (B) in adult SHR ventricular myocytes. Each panel shows three pairs of confocal images of the same myocyte: bottom surface, center (~ 4 um from either surface), and top surface. Upper row depicts intrinsic fluorescence signals from Q1-GFP or E1-dsR protein. Lower row depicts fluorescence signals from probes bound to Q1-GFP or E1-dsR mRNA.

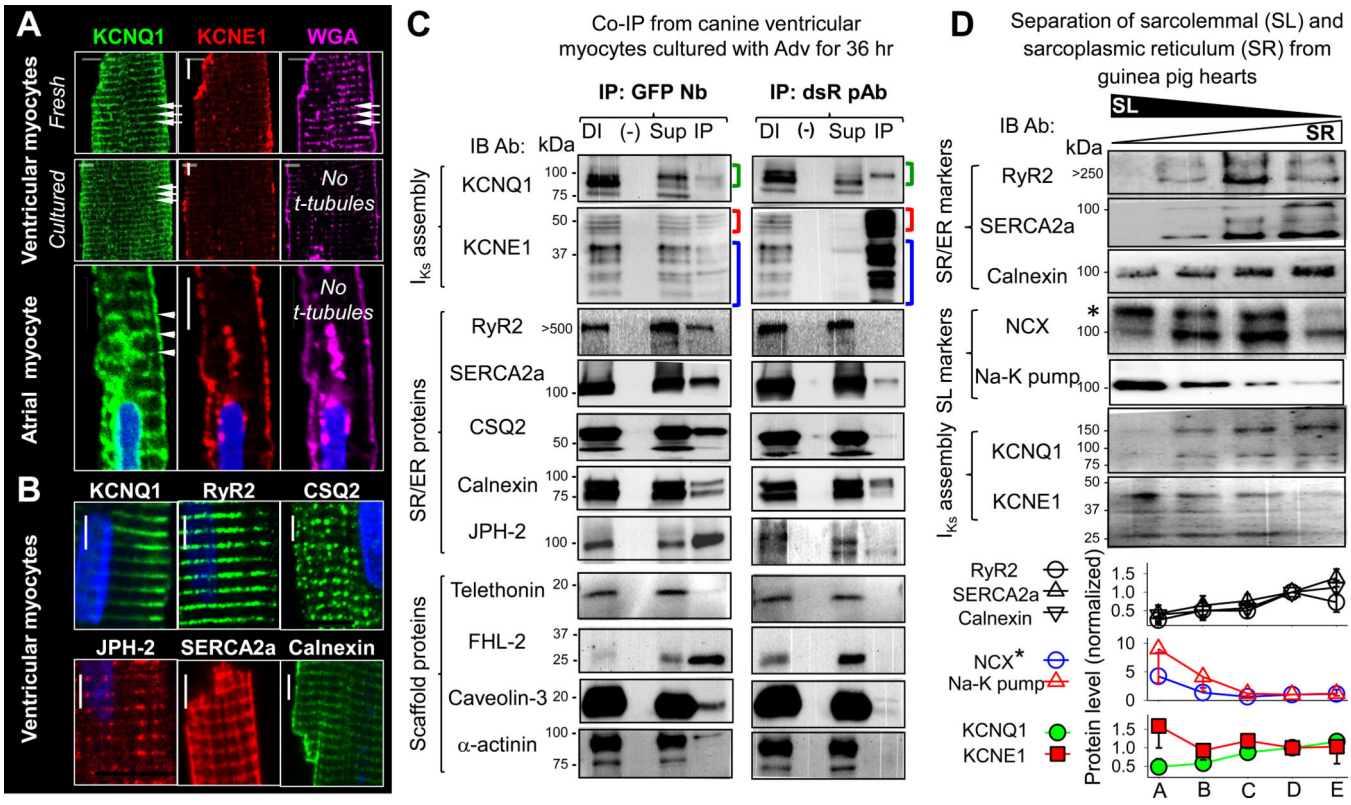


**Figure 5.**

Probing KCNQ1 and KCNE1 subcellular compartments in adult cardiac myocytes. (**A**) Q1 exhibits clear striations in myocytes where t-tubules (striations in WGA signals) are missing. *Top 2 rows*: CVMs from same heart fixed right after isolation 'Fresh', or after 48-hr culture 'Cultured'. *Bottom*: Images from atrial myocyte. Arrowheads point to Q1 striations and corresponding positions in WGA image. In all cases, E1 is detected on peripheral surface. (**B**) Q1 striations overlap with those of SR markers. Scale bars = 5 um. (**C**) Q1-GFP coimmunoprecipitates with SR proteins, while E1-dsR cannot. Whole cell lysates (WCLs) from CVMs incubated for 36 hr with Adv-Q1-GFP and Adv-E1-dsR are subjected to immunoprecipitation with GFP nanobody (GFP Nb, left column) or dsR rabbit pAb (right column). Each panel shows four lanes: 'DI' - direct input (WCL, as positive control), (−) – negative control (eluent from control agarose beads incubated with WCL), 'Sup' – supernatant (WCL after immunoprecipitation), and 'IP' – immunoprecipitate (eluent from immunoprecipitating Ab-conjugated beads incubated with WCL). Abs used in immunoblot 'IB' and size marker positions listed on left. Green, red and blue brackets denote Q1-GFP, E1-dsR and native E1 bands (band validation in Fig. S1A). (**D**) Native Q1 protein is enriched in SR compartment, while E1 is enriched in SL. *Upper*: Immunoblot images of lysates from Ca-oxalate loaded membrane vesicles prepared from guinea pig hearts and separated by sucrose gradients (left to right: light-to-heavy vesicles) probed for SR and SL markers, Q1 and E1 (listed on left, *glycosylated NCX band). *Lower*: Densitometry quantification of band intensities. Data are pooled from 3 – 6 immunoblots, each normalized by the band intensity in fraction 'D'. In this and the following figures, pooled data are presented as mean ±SE.

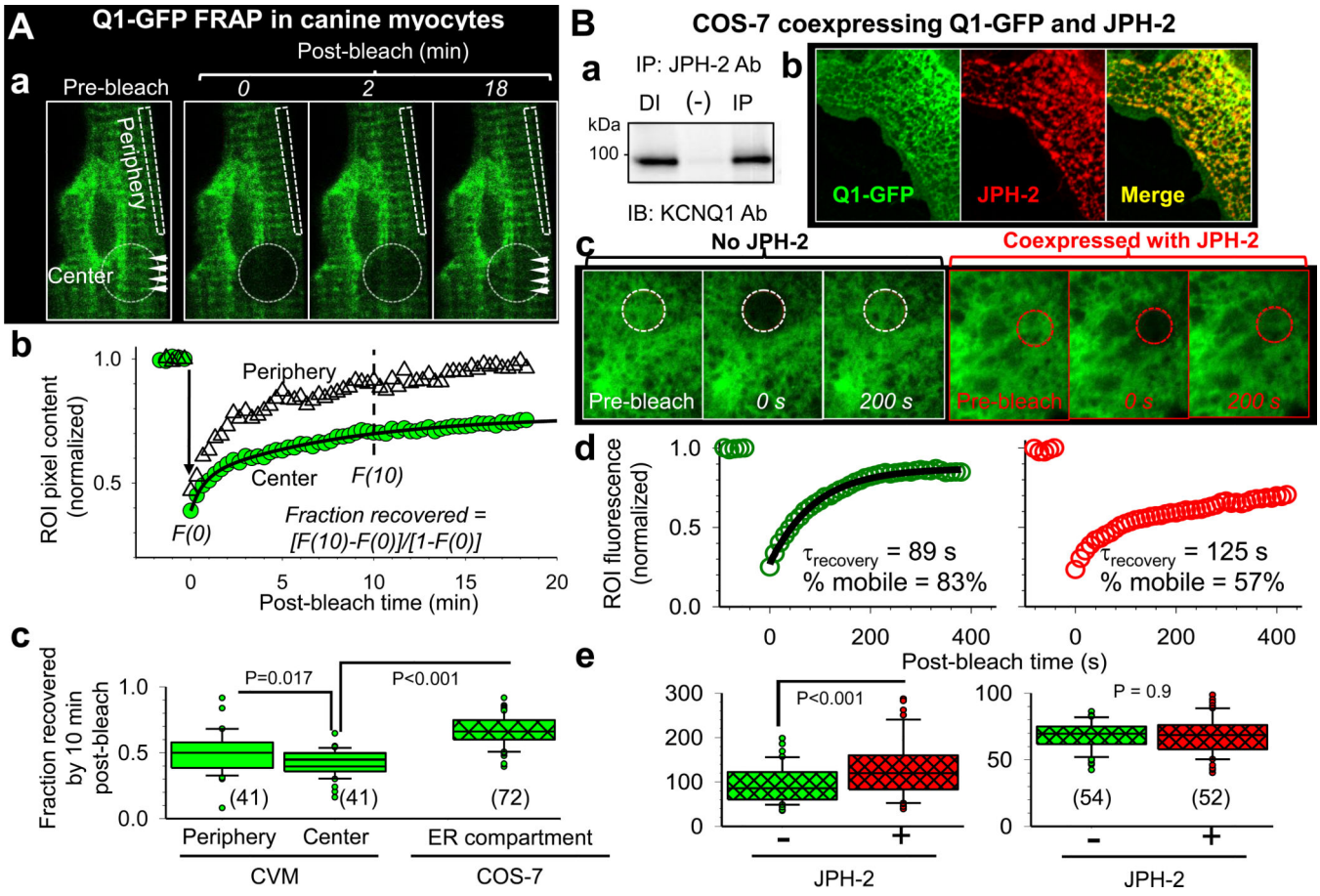


**Figure 6.**

Probing Q1-GFP mobility by fluorescence-recovery-after-photobleaching (FRAP). (**A**) FRAP of Q1-GFP expressed in canine ventricular myocytes (CVM). ‘a’: Q1-GFP images before and after photobleaching two regions of interest (ROI): circular ROI in myocyte center ‘Center’, and rectangle ROI along peripheral surface ‘Periphery’. White arrowheads mark striations before and after recovery from photobleaching. ‘b’: Time courses of changes in fluorescence intensity (pixel contents, normalized by values before photobleaching) in the two ROIs. Data points are superimposed on double-exponential best-fit curves. *Inset*: calculation of fraction recovered by 10 min post-bleach; F(0) and F(10) are pixel contents at time zero and 10 min post-bleach illustrated by arrow and dotted line. ‘c’: Box plots of fraction recovered by 10 min post-bleach in the specified compartments of CVM (from 4 animals) and COS-7 cells. (**B**) Effects of JPH-2 on Q1-GFP mobility in COS-7 ER compartment. ‘a’: JPH-2 co-immunoprecipitates with Q1-GFP. ‘b’: Puncta of JPH-2 immunofluorescence overlap with Q1-GFP in ER reticulum. ‘c’: Q1-GFP images before and after photobleaching when expressed alone or with JPH-2. Bleached ROIs are marked by circles. ‘d’: Time courses of fluorescence recovery from the same cells as shown in ‘c’. The recovery phase is fit with a single-exponential function, with time constant of fluorescence recovery ($\tau_{recovery}$) and Q1-GFP mobile fraction (% mobile) marked. ‘e’: Comparing $\tau_{recovery}$ and % mobile of Q1-GFP expressed alone or with JPH-2. (n): number of ROIs analyzed.

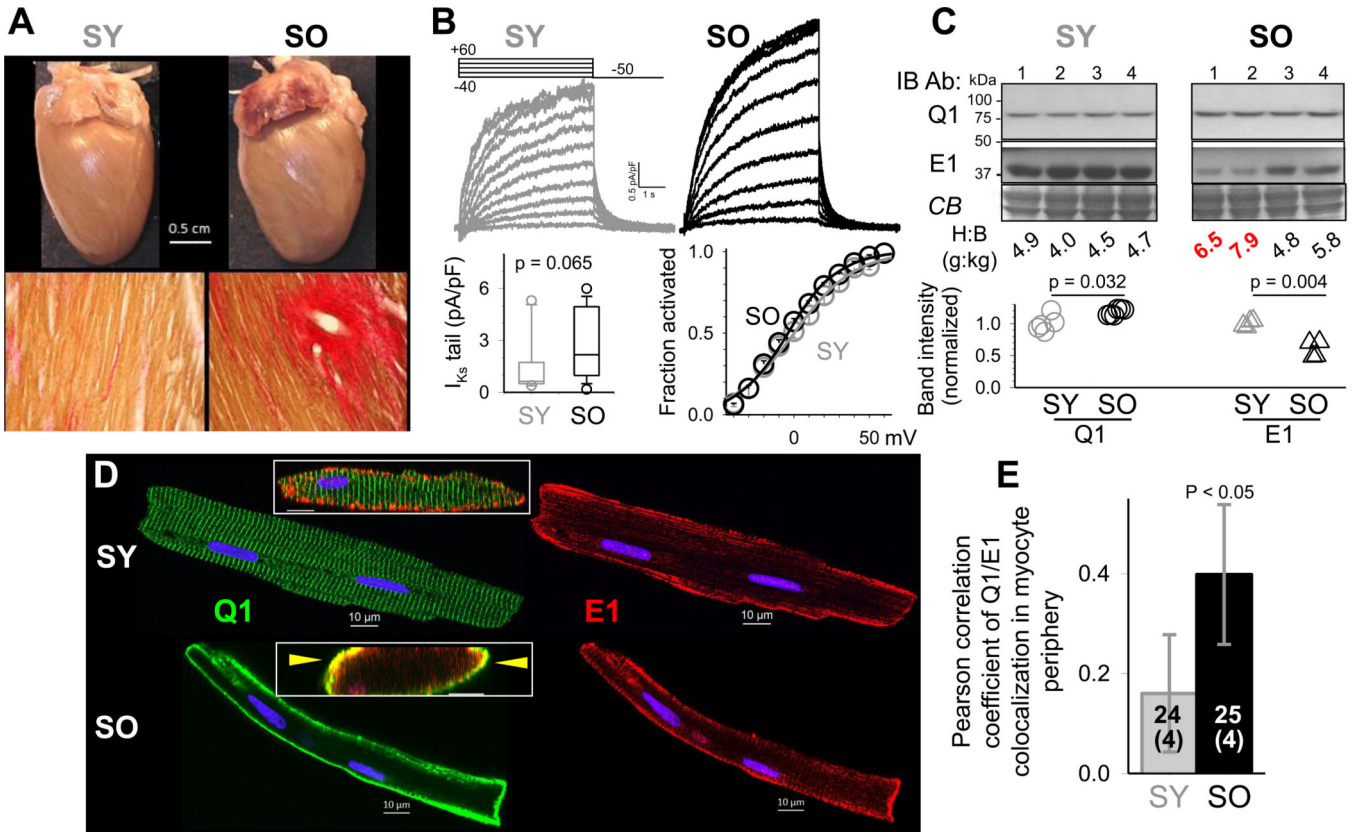


**Figure 7.**

Persistent localization of native KCNQ1 to the peripheral cell surface in chronically stressed adult ventricular myocytes. Young and old SHR (SY and SO) are 4–6 and 22–24 months of age. (**A**) *Top*: SY and SO hearts and LV stained with van Gieson's dyes (yellow: myocytes, red: fibrotic tissue). (**B**) Patch clamp recordings from SY and SO LV Epi myocytes. *Top*: HMR1556-sensitive ($I_{Ks}$) currents. *Bottom left*: $I_{Ks}$ densities (10 and 14 myocytes each from 4 SY and 4 SO hearts). *Bottom right*: Activation curves of $I_{Ks}$ in SY and SO myocytes. (**C**) Immunoblot quantification of Q1 and E1 proteins in SY and SO LV samples. *Top*: Q1 and E1 immunoblot images. Coomassie-blue stain (CB) confirms even loading among lanes. Heart-to-body weight ratios (H:B, in g:kg) noted below. Red highlights two SO animals in heart failure. *Bottom*: densitometry quantification of Q1 and E1 proteins in SY and SO LV samples, normalized by the mean values of SY samples. (**D**) Distribution of native Q1 and E1 in SY and SO LV myocytes. *Main graph*: Confocal immunofluorescence images. *Inset*: Oblique cross-section of merged Q1 and E1 signals; arrowheads point to Q1/E1 overlaps. **(E)** Q1/E1 colocalization in myocyte periphery quantified by thresholded Pearson correlation coefficient, measured from 24 SY and 25 SO myocytes of 4 animals each. Bars represent 95% confidence interval.

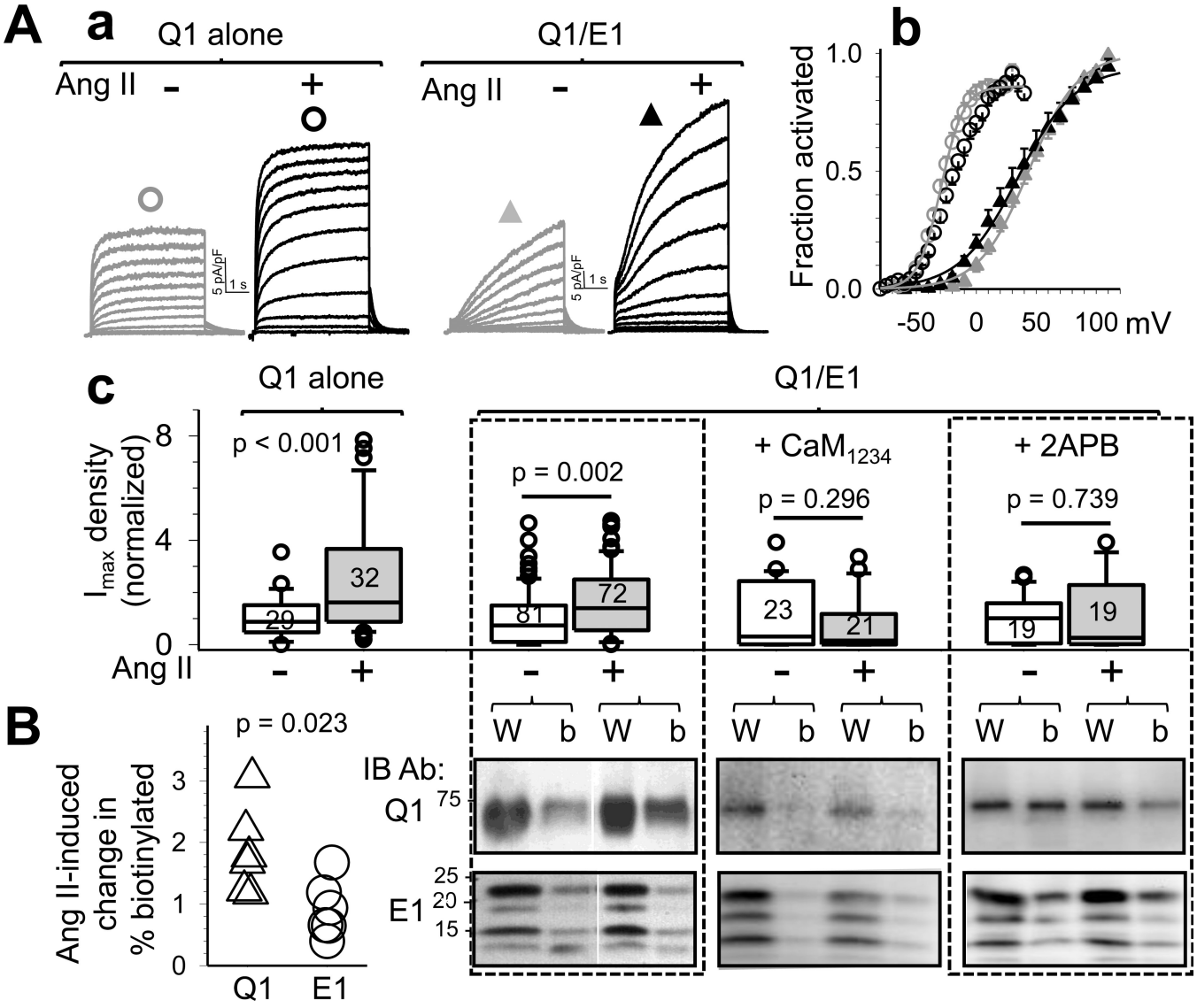


**Figure 8.**

Persistent activation of angiotensin-type 1-receptor (AT1R) induces KCNQ1 trafficking to cell surface via a Ca- and calmodulin-dependent mechanism. COS-7 cells are transfected with AT1R and Q1, Q1/E1, or Q1/E1 plus Ca-binding-deficient calmodulin ($CaM_{1234}$), pretreated with Ang II (1 uM, 36°C, 1 hr) or without (+ or –Ang II), in presence or absence of 5 uM 2APB. Experiments are conducted in the absence of Ang II. (**A**) Patch clamp data. 'a': Current traces from Q1 or Q1/E1 cells without or with Ang II pretreatment. 'b': Activation curves from four groups of cells noted by same symbols as shown above current traces in 'a'. 'c': Summarized $I_{max}$ density normalized by mean values from '–Ang II' cells. Number of cells patch clamped noted in boxes. (**B**) Ang II incubation-induced change in % biotinylatied fraction of Q1 and E1. *Right*: Immunoblot images of Q1 (top) and E1 (bottom) of whole cell lysates (W) and biotinylated fraction (b). *Left*: Summary of % biotinylated Q1 and E1 normalized by '-Ang II' data, n=6.